Journal of Sound and Vibration (2002) **252**(4), 675–696
doi:10.1006/jsvi.2001.4050 available online at http://www.idealibrary.com on IDEAL®

NON-LINEAR STEADY STATE VIBRATIONS OF BEAMS EXCITED BY VORTEX SHEDDING

R. Lewandowski

Poznan University of Technology, Institute of Structural Engineering, 60-965 Poznan, 5 Piotrowo Street, Poland. E-mail: roman.lewandowski@put.poznan.pl

(*Received* 18 *October* 1999, *and in final form* 23 *August* 2001)

In this paper the non-linear vibrations of beams excited by vortex-shedding are considered. In particular, the steady state responses of beams near the synchronization region are taken into account. The main aerodynamic properties of wind are described by using the semi-empirical model proposed by Hartlen and Currie. The finite element method and the strip method are used to formulate the equation of motion of the system treated. The harmonic balance method is adopted to derive the amplitude equations. These equations are solved with the help of the continuation method which is very convenient to perform the parametric studies of the problem and to determine the response curve in the synchronization region. Moreover, the equations of motion are also integrated using the Newmark method. The results of calculations of several example problems are also shown to confirm the efficiency and accuracy of the presented method. The results obtained by the harmonic balance method and by the Newmark methods are in good agreement with each other.

1. INTRODUCTION

The effects of wind action on structures are vibrations of different kinds. Some of them can be dangerous for the safety of structures. Slender structures like steel chimneys, bridge pylons and guyed masts are examples of structures which are very sensitive to wind-induced vibrations. One type of such dangerous vibrations is known as the lock-in phenomenon. The effects of these vibrations are the results of wind passing across a bluff body and forming an aerodynamic wake. In a flowing fluid, vortices are shed alternately from either side of the body, and the resulting changes in circulation around the body lead to fluctuating forces. As the frequency of shedding ω_s is approximately equal to one of the natural frequencies of structures ω_n, the structure often vibrates with large amplitudes in a plane perpendicular to the flow direction. Vortex-induced vibrations are found to be amplitude dependent, self-limiting and very sensitive to the structural damping level. As it is clearly shown in many papers describing the results of experimental works (written, for example, by Brika and Laneville [1] and Goswami *et al.* [2]) in the synchronization range (i.e., when $\omega_s \approx \omega_n$), the vibrations of structures are periodic and modulated outside this range. In the lock-in range the oscillation of the body takes control of the shedding and the feedback of the affected flow field may, in turn, reinforce the vibrations.

The investigations of the lock-in phenomenon, which is complex, requires advanced theoretical models, e.g., Navier–Stokes equations, but the computational requirements of these models strongly limit their applications. Due to the complicated process of simulation of vortex shedding phenomena, empirical models are often used in civil

0022-460X/02/$35.00

engineering because one is mainly interested in the maximum vortex-induced response of structures and the details concerning the flow are less important. Therefore, empirical or semi-empirical models that provide a reasonable approximation of the aeroelastic response are used. There are a number of models of this kind. Generally speaking, almost all these models are non-linear and deterministic or stochastic. The most popular stochastic model proposed by Vickery and Basu [3] takes into account the probabilistic character of the wind excitation forces. Recently, a new model of this kind is proposed by Flaga [4].

Deterministic models fall into two main categories. The basic idea of the first model is that the fluid is associated with an internal degree of freedom that interacts with the structural elements in the form of two coupled oscillators. The models of this kind are proposed by Hartlen and Currie [5], Iwan and Blevins [6] and by Landle [7]. The Hartlen–Currie model was modified by Skop and Griffin [8] who introduced a non-linear spring stiffness. However, the experiments by Oey *et al.* [9], set up specifically to identify the effect of non-linear stiffness, concluded that the response of a cylinder was insensitive to this effect. Recently, a very interesting model was presented by Krenk and Nielsen [10]. Another class of models proposed by Simiu and Scanlan [11], Vickery and Basu [3], Goswami *et al.* [12] and Larsen [13] describes the phenomenon by a single equation of motion in which aeroelastic forcing terms are included.

At the present time it is hard to say which model is the best. Each model has its own advantages and disadvantages. For example, in the Vickery and Basu model the so-called correlation length of the aerodynamic forces can be taken into account in a natural way. However, in the deterministic models, the correlation length cannot be easily introduced because of the stochastic character of this quantity. An empirical formula which approximately describe the correlation length in terms of amplitudes of vibration is proposed by Ruschaweyh [14].

Despite its own limitation the model proposed by Harten and Currie is often used as the one which seems to be in quite good agreement with the experimental data.

The problem of vortex-induced vibrations of beams was analyzed previously by Baroush *et al.* [15] and Dul and Pietrucha [16], who used semi-empirical aerodynamic models and time integration methods to determine the steady state vibration of beams. This approach requires an extremely high computational effort because of small system damping. However, the computational cost can be drastically reduced by using the harmonic balance method as shown by Lewandowski [17] for the semi-empirical models proposed by Simiu and Scanlan [18] and by Goswami *et al.* [12].

In the present paper, the strips and finite element methods together with the Hartlen–Currie type vortex shedding model are used in a parametric analysis of vortex-induced vibrations of beams in a synchronization region.

2. BRIEF DESCRIPTION OF HARTLEN–CURRIE MODEL

In reference [5] an elastically supported, rigid cylinder in air flow is considered. The cylinder motion is restricted to pure translation in the direction perpendicular to the flow direction and the cylinder axis. The equations of motion for this model are derived in the following non-dimensional form:

$$\ddot{w} + 2\xi\dot{w} + w = a\omega_s^2 c_L, \tag{1}$$

$$\ddot{c}_L - \alpha\omega_s\dot{c}_L + \gamma\dot{c}_L^3/\omega_s + \omega_s^2 c_L = b\omega_n\dot{w}, \tag{2}$$

where, $w, c_L, \xi, \omega_s, \alpha, \gamma, a, b$ are the cylinder displacement, the "hidden" aerodynamic variable interpreted as the lift coefficient, the damping factor for the cylinder, the non-dimensional shedding frequency which is proportional to the wind mean velocity U and some aerodynamic constants respectively. The differentiation with respect to time is denoted by a dot. The aerodynamic constants α, γ, a, b are determined experimentally. Equation (2) is the non-linear, van der Pol differential equation. From the mathematical point of view this equation could be understood as the equation of motion of a fictitious mechanical oscillator with a non-linear damping characteristic. More detailed description of the above model is given in reference [5]. In the next section, the Hartlen–Currie model will be extended to beams treated as systems with multi degrees of freedom.

3. DESCRIPTION OF COMPUTATIONAL MODEL

The finite element method has received broad acceptance as the convenient analysis tool in structural engineering because this method allows detailed computations of the response and stress distributions in structural members subjected to loads. In this work, the well-known displacement version of finite element method is used to developed a discrete model of a beam. This approach to considered particular problem is more adequate than very popular modal ones because the influence of more then one mode of vibration can be taken into account in an easy way. As shown in many papers (see, for example references [19-22]), the interaction of two or more modes of vibration could be very important if non-linear systems are considered. Moreover, beams with the non-uniform spatial distribution of the beam bending stiffness, the mass per unit length or the cross-section characteristic dimension can be modelled more accurately.

The considered system (the beam and the flow field) is divided into finite elements (beam) and strips (flow field). Each strip is parallel to the direction of the undisturbed flow and has a width equal to the finite element length. The strips are also perpendicular to the finite elements. The main assumption is that flows in strips are mutually independent, which means that the aerodynamic forces are induced only by the flow in the associated strip.

In this article, two types of descriptions of the lift factor $c_L(x, t)$ along the strip width are taken into account. In Case 1, the distribution of the lift coefficient $c_L(x, t)$ along the strip width is a linear function of the nodal parameter and it is assumed that

$$c_L(x, t) = \mathbf{N}_L^{\mathrm{T}}(x)\mathbf{c}_e(t), \tag{3}$$

where $\mathbf{N}_L(x) = col(N_1(x), N_2(x))$, $N_1(x) = 1 - \eta$, $N_2(x) = \eta$, $\eta = x/l$, $\mathbf{c}_e = col(c_a, c_b)$ are the vector of shape functions and the vector of nodal parameters of the strip respectively. Moreover, in the Case 2, it is assumed that the lift factor is constant along the strip. Thus, one can formally write $\mathbf{N}_L(x) = col(N_1(x))$, $N_1(x) = 1$, and $\mathbf{c}_e = col(c)$.

The cross-wind transverse displacements $w(x, t)$ of the typical two-node beam finite element with two degrees of freedom per node are described using the Hermitan polynomial shape functions, i.e.,

$$w(x, t) = \mathbf{N}_b^{\mathrm{T}}(x)\mathbf{w}_e(t), \tag{4}$$

where $\mathbf{N}_b(x) = col(N_3(x), N_4(x), N_5(x), N_6(x))$ and $\mathbf{w}_e(t) = col(w_a, \phi_a, w_b, \phi_b)$ are the vector of beam shape functions and the vector of nodal parameters respectively.

The kinetic and strain energy of the finite element can be written in the form

$$K_b^e = \tfrac{1}{2}\dot{\mathbf{w}}_e^{\mathrm{T}}\mathbf{M}_b^e\dot{\mathbf{w}}_e, \qquad W_b^e = \tfrac{1}{2}\mathbf{w}_e^{\mathrm{T}}\mathbf{K}_b^e\mathbf{w}_e, \tag{5}$$

where $\mathbf{M}_b^e$ and $\mathbf{K}_b^e$ are the well-known mass and stiffness matrices respectively.

The virtual work of non-conservative forces acting on the finite element consists of the damping term and external excitation term. The damping term is represented by

$$\delta L_{bd}^e = \delta\mathbf{w}_e^{\mathrm{T}}\mathbf{D}_b^e\dot{\mathbf{w}}_e, \tag{6}$$

where the $\mathbf{D}_b^e$ damping matrix is given by $\mathbf{D}_b^e = \kappa_1\mathbf{M}_b^e + \kappa_2\mathbf{K}_b^e$ and κ_1 and κ_2 are some constants. It means that the so-called proportional damping model is taken into account.

The aerodynamic external forces $f(x,t)$ acting on the beam are given by

$$f(x,t) = \tfrac{1}{2}\rho U^2(x)D(x)c_L(x,t), \tag{7}$$

where the $\rho, U(x), D(x)$ symbols denote the air density, the mean velocity of wind and the cross-section characteristic dimension respectively. The distribution of mean wind velocity along the beam could be represented as a product of the reference wind velocity denoted by U and the function of the wind profile $p(x)$ i.e., $U(x) = Up(x)$. In a similar way, the non-dimensional characteristic cross-section dimension $d(x)$ is defined as $d(x) = D(x)/D$, where D is the reference characteristic cross-section dimension. However, in this paper, it is assumed that $U(x)$ and $D(x)$ are constant along the length of the finite element. It means that $p(x) = p_e$ and $d(x) = d_e$ are also constant.

The virtual work of aerodynamic forces can be written as

$$\int_{t_1}^{t_2}\delta L_{ba}^e\,\mathrm{d}t = \int_{t_1}^{t_2}\int_0^l \delta w(x)f(x,t)\,\mathrm{d}x\,\mathrm{d}t = \int_{t_1}^{t_2}\omega_s^2\delta\mathbf{w}_e^{\mathrm{T}}\mathbf{S}_L^e\mathbf{c}_e(t)\,\mathrm{d}t, \tag{8}$$

where the $\mathbf{S}_L^e$ matrix is defined by

$$\mathbf{S}_L^e = \frac{\rho D^3 p_e^2 d_e}{8\pi^2 S^2}\int_0^l \mathbf{N}_b(x)\mathbf{N}_L^{\mathrm{T}}(x)\,\mathrm{d}x. \tag{9}$$

Moreover, $\omega_s = 2\pi SU/D$, S is the Stouhal number and l is the length of the finite element.

After integration the elements of the $\mathbf{S}_L^e$ matrix are

in Case 1

$$\mathbf{S}_L^e = \frac{D^3 p_e^2 d_e l}{8\pi^2 S^2}\begin{bmatrix} \frac{7}{20} & \frac{3}{20} \\ \frac{l}{20} & \frac{l}{30} \\ \frac{3}{20} & \frac{7}{20} \\ -\frac{l}{30} & -\frac{l}{20} \end{bmatrix}, \tag{10a}$$

whereas in Case 2

$$\mathbf{S}_L^e = \frac{D^3 p_e^2 d_e l}{8\pi^2 S^2}\,col\left(\frac{1}{2}, \frac{l}{12}, \frac{1}{2}, -\frac{l}{12}\right). \tag{10b}$$

The Hartlen–Currie model describes, by equation (2), the motion of some artificial variable (i.e., the motion of the lift factor) which characterizes the flow action in a global way. This equation takes into account only the primary characteristic deduced from experiments. However, many details connected with the flow are omitted. From the mathematical point of view the above mentioned equation could be understood as the

equation of motion of a fictitious mechanical oscillator with a non-linear damping characteristic. In order to make possible the weak formulation for the whole system the "kinetic and strain energy" and the "virtual work of non-conservative forces" for the fictitious oscillators are also introduced in this article. Obviously, these quantities must be considered as specific functionals, which leads one to the counterparts of the second equation of the Hartlen–Currie model in the case of systems with many degrees of freedom. The 'kinetic and strain energy' for the lift coefficient is defined as follows

$$K_L^e = \int_0^l \tfrac{1}{2}\dot{c}_L^2(x,t)\,\mathrm{d}x = \tfrac{1}{2}\dot{\mathbf{c}}_e^{\mathrm{T}}\mathbf{M}_L^e\dot{\mathbf{c}}_e, \qquad W_L^e = \int_0^l \tfrac{1}{2}\omega_s^2 c_L^2(x,t)\,\mathrm{d}x = \tfrac{1}{2}\omega_s^2\mathbf{c}_e^{\mathrm{T}}\mathbf{K}_L^e\mathbf{c}_e, \quad (11)$$

where the matrices

$$\mathbf{M}_L^e = \int_0^l \mathbf{N}_L(x)\mathbf{N}_L^{\mathrm{T}}(x)\,\mathrm{d}x, \qquad \mathbf{K}_L^e = \frac{p_e^2}{d_e^2}\int_0^l \mathbf{N}_L(x)\mathbf{N}_L^{\mathrm{T}}(x)\,\mathrm{d}x, \quad (12)$$

are the "mass" and "stiffness" matrices of introduced fictitious aerodynamic oscillators.

After integration these matrices can be written in the following form:
in Case 1

$$\mathbf{M}_L^e = l\begin{bmatrix}\frac{1}{3} & \frac{1}{6}\\ \frac{1}{6} & \frac{1}{3}\end{bmatrix}, \qquad \mathbf{K}_L^e = \frac{p_e^2}{d_e^2}l\begin{bmatrix}\frac{1}{3} & \frac{1}{6}\\ \frac{1}{6} & \frac{1}{3}\end{bmatrix}, \quad (13a)$$

where as in Case 2

$$\mathbf{M}_L^e = l[1], \qquad \mathbf{K}_L^e = \frac{p_e^2}{d_e^2}l[1]. \quad (13b)$$

The 'virtual work of the damping forces' for the 'hidden variable' is defined by

$$\int_{t_1}^{t_2}\int_0^l \delta c_L(x)(-\alpha\omega_s\dot{c}_L(x,t) + \gamma\dot{c}_L^3(x,t)/\omega_s)\,\mathrm{d}x\,\mathrm{d}t$$
$$= \int_{t_1}^{t_2}\delta\mathbf{c}_e^{\mathrm{T}}[-\omega_s\mathbf{D}_L^e + \omega_s^{-1}\mathbf{D}_{NL}^e(\dot{\mathbf{c}}_e,\dot{\mathbf{c}}_e)]\dot{\mathbf{c}}_e(t)\,\mathrm{d}t, \quad (14)$$

where

$$\mathbf{D}_L^e = \frac{\alpha_e p_e}{d_e}\int_0^l \mathbf{N}_L(x)\mathbf{N}_L^{\mathrm{T}}(x)\,\mathrm{d}x, \quad (15)$$

$$\mathbf{D}_{NL}^e(\dot{\mathbf{c}}_e,\dot{\mathbf{c}}_e) = \frac{\gamma_e d_e}{p_e}\int_0^l \mathbf{N}_L^{\mathrm{T}}(x)\dot{\mathbf{c}}_e(t)\dot{\mathbf{c}}_e^{\mathrm{T}}(t)\mathbf{N}_L(x)\mathbf{N}_L(x)\mathbf{N}_L^{\mathrm{T}}(x)\,\mathrm{d}x. \quad (16)$$

After integration, the $\mathbf{D}_L^e$ matrix can be written in the following form:
in Case 1

$$\mathbf{D}_L^e = \frac{\alpha_e p_e l}{d_e}\begin{bmatrix}\frac{1}{3} & \frac{1}{6}\\ \frac{1}{6} & \frac{1}{3}\end{bmatrix}, \quad (17a)$$

in Case 2

$$\mathbf{D}_L^e = \frac{\alpha_e p_e l}{d_e}[1]. \quad (17b)$$

The $\mathbf{D}^e_{NL}(\dot{\mathbf{c}}_e, \dot{\mathbf{c}}_e)$ non-linear damping matrix is a quadratic function of velocity of nodal parameters. The elements of this matrix are denoted by d_{ij} and can also be written in the explicit form given below

in Case 1

$$d_{11} = \frac{\gamma_e d_e l}{p_e}\left(\frac{1}{5}c_a^2 + \frac{1}{10}c_a c_b + \frac{1}{30}c_b^2\right),$$

$$d_{12} = d_{21} = \frac{\gamma_e d_e l}{p_e}\left(\frac{1}{20}c_a^2 + \frac{1}{15}c_a c_b + \frac{1}{20}c_b^2\right),$$

$$d_{22} = \frac{\gamma_e d_e l}{p_e}\left(\frac{1}{30}c_a^2 + \frac{1}{10}c_a c_b + \frac{1}{5}c_b^2\right), \tag{18a}$$

in Case 2

$$d_{11} = \frac{\gamma_e d_e l}{p_e}c^2. \tag{18b}$$

In the above relations the α_e and γ_e symbols denote the constants which must be determined experimentally and they can be different for each strip.

The 'virtual work of external forces' associated with the fictitious oscillators is defined by

$$\int_{t_1}^{t_2} \delta L_{Le}\,\mathrm{d}t = \int_{t_1}^{t_2}\int_0^l \delta c(x) b_e \dot{w}(x,t)\,\mathrm{d}x\,\mathrm{d}t = \int_{t_1}^{t_2} \delta \mathbf{c}_L^{\mathrm{T}} \mathbf{S}_b^e \dot{\mathbf{w}}_e(t)\,\mathrm{d}t, \tag{19}$$

where

$$\mathbf{S}_b^e = b_e \int_0^l \mathbf{N}_L(x)\mathbf{N}_b^{\mathrm{T}}(x)\,\mathrm{d}x. \tag{20}$$

The explicit form of the $\mathbf{S}_b^e$ matrix is given by

in Case 1

$$\mathbf{S}_b^e = b_e l \begin{bmatrix} \frac{7}{20} & \frac{l}{20} & \frac{3}{20} & -\frac{l}{30} \\ \frac{3}{20} & \frac{l}{30} & \frac{7}{20} & -\frac{l}{20} \end{bmatrix} \tag{21a}$$

and in Case 2

$$\mathbf{S}_b^e = b_e l \left[\frac{1}{2}, \frac{l}{12}, \frac{1}{2}, -\frac{l}{12}\right]. \tag{21b}$$

Here b_e is the experimentally determined aerodynamic constant. The equation of motion of the original Hartlen–Currie model is described using the non-dimensional time $\tau = \omega_n t$, where ω_n is the natural frequency of the cylinder. In this paper, we do not deal with non-dimensional time. For this reason, our definition of the b_e constant is $b_e = \omega_n b_{HC}$, where b_{HC} is the b constant as defined by Hartlen and Currie and now ω_n denotes the natural frequency near which the synchronization region is currently analyzed.

The equations of motion are derived on basis of the Hamilton principle, which states that

$$\int_{t_1}^{t_2} [\delta(K - W) + \delta L]\,\mathrm{d}t = 0, \tag{22}$$

where δ is the variational operator and K, W and δL denote the total kinetic and strain energy of the system and the virtual work of non-conservative forces respectively. Using the Hamilton principle one can derive the following equations of motion for the typical beam element and strip respectively

$$\mathbf{R}_b^e = \mathbf{M}_b^e \ddot{\mathbf{w}}_e(t) + \mathbf{D}_b^e \dot{\mathbf{w}}_e(t) + \mathbf{K}_b^e \mathbf{w}_e(t) - \omega_s^2 \mathbf{S}_L^e \mathbf{c}_e(t), \tag{23}$$

$$\mathbf{R}_L^e = \mathbf{M}_L^e \ddot{\mathbf{c}}_e(t) - \omega_s \mathbf{D}_L^e \dot{\mathbf{c}}_e(t) + \omega_s^{-1} \mathbf{D}_{NL}^e(\dot{\mathbf{c}}_e(t), \dot{\mathbf{c}}_e(t))\dot{\mathbf{c}}_e(t) + \omega_s^2 \mathbf{K}_L^e \mathbf{c}_e(t) - \mathbf{S}_b^e \dot{\mathbf{w}}_e(t). \tag{24}$$

After the assembly procedure the equations of motion for the entire system can be written as

$$\mathbf{R}_b(t) = \mathbf{M}_b \ddot{\mathbf{w}}(t) + \mathbf{D}_b \dot{\mathbf{w}}(t) + \mathbf{K}_b \mathbf{w}(t) - \omega_s^2 \mathbf{S}_L \mathbf{c}(t) = \mathbf{0}, \tag{25}$$

$$\begin{aligned} \mathbf{R}_L(t) = {} & \mathbf{M}_L \ddot{\mathbf{c}}(t) - \omega_s \mathbf{D}_L \dot{\mathbf{c}}(t) + \omega_s^{-1} \mathbf{D}_{NL}(\dot{\mathbf{c}}(t), \dot{\mathbf{c}}(t))\dot{\mathbf{c}}(t) \\ & + \omega_s^2 \mathbf{K}_L \mathbf{c}(t) - \mathbf{S}_b \dot{\mathbf{w}}(t) = \mathbf{0}, \end{aligned} \tag{26}$$

where $\mathbf{M}_b, \mathbf{M}_L, \mathbf{D}_b, \mathbf{D}_L, \mathbf{D}_{NL}(\dot{\mathbf{c}}(t), \dot{\mathbf{c}}(t)), \mathbf{K}_b, \mathbf{K}_L, \mathbf{S}_b, \mathbf{S}_L, \mathbf{w}(t), \mathbf{c}(t)$ are the global counterparts of previously defined, matrices and vectors on a level of element and strip. The $\mathbf{R}_b(t)$ and $\mathbf{R}_L(t)$ residual vectors vanish in an equilibrium state.

4. DERIVATION OF AMPLITUDE EQUATIONS

The steady state, periodic response of the system can be described in a first approximation by

$$\mathbf{w}(t) = \mathbf{w}_c \cos \omega t + \mathbf{w}_s \sin \omega t, \qquad \mathbf{c}(t) = \mathbf{c}_c \cos \omega t + \mathbf{c}_s \sin \omega t, \tag{27}$$

where $\mathbf{w}_c, \mathbf{w}_s, \mathbf{c}_c, \mathbf{c}_s$ are the unknown vectors of harmonic amplitudes of nodal parameters of beam and strips on a level of the entire system and the finite element and strip respectively. Also, the frequency of oscillation ω is an unknown quantity. In this paper, the solution with only one harmonic is taken into account because the results of experiments show that it is accurate enough in the synchronization region.

The solutions of the equations of motion on a finite element level and on a strip level are given in a similar way:

$$\mathbf{w}_e(t) = \mathbf{w}_{ce} \cos \omega t + \mathbf{w}_{se} \sin \omega t, \qquad \mathbf{c}_e(t) = \mathbf{c}_{ce} \cos \omega t + \mathbf{c}_{se} \sin \omega t. \tag{28}$$

The in-time Galerkin procedure is used to derive the amplitude equations. These equations follow from the Galerkin conditions which state that

$$\frac{2}{T}\int_0^T \mathbf{R}_b(t)\cos \omega t \, \mathrm{d}t = \mathbf{0}, \qquad \frac{2}{T}\int_0^T \mathbf{R}_b(t)\sin \omega t \, \mathrm{d}t = \mathbf{0},$$

$$\frac{2}{T}\int_0^T \mathbf{R}_L(t)\cos \omega t \, \mathrm{d}t = \mathbf{0}, \qquad \frac{2}{T}\int_0^T \mathbf{R}_L(t)\sin \omega t \, \mathrm{d}t = \mathbf{0}, \tag{29}$$

where $T = 2\pi/\omega$ denotes the unknown period of the limit cycle. The $\mathbf{R}_b(t)$ and $\mathbf{R}_L(t)$ residual vectors appearing in equations (29) are determined by introducing the assumed solution of motion equations into equations (25) and (26). After calculating the resulting integrals from the Galerkin conditions, one obtains the following set of non-linear

algebraic equations with respect to $\mathbf{w}_c, \mathbf{w}_s$, $\mathbf{c}_c$ and $\mathbf{c}_s$:

$$(\mathbf{K}_b - \omega^2\mathbf{M}_b)\mathbf{w}_c + \omega\mathbf{D}_b\mathbf{w}_s - \omega_s^2\mathbf{S}_L\mathbf{c}_c = \mathbf{0}, \tag{30}$$

$$-\omega\mathbf{D}_b\mathbf{w}_c + (\mathbf{K}_b - \omega^2\mathbf{M}_b)\mathbf{w}_s - \omega_s^2\mathbf{S}_L\mathbf{c}_s = \mathbf{0}, \tag{31}$$

$$\begin{aligned}&(\omega_s^2\mathbf{K}_L - \omega^2\mathbf{M}_L)\mathbf{c}_c - \omega\omega_s\mathbf{D}_L\mathbf{c}_s \\ &+ \tfrac{3}{4}\omega^3\omega_s^{-1}[\mathbf{D}_{NL}(\mathbf{c}_c, \mathbf{c}_c) + \mathbf{D}_{NL}(\mathbf{c}_s, \mathbf{c}_s)]\mathbf{c}_s - \omega\mathbf{S}_b\mathbf{w}_s = \mathbf{0},\end{aligned} \tag{32}$$

$$\begin{aligned}&\omega\omega_s\mathbf{D}_L\mathbf{c}_c - \tfrac{3}{4}\omega^3\omega_s^{-1}[\mathbf{D}_{NL}(\mathbf{c}_c, \mathbf{c}_c) + \mathbf{D}_{NL}(\mathbf{c}_s, \mathbf{c}_s)]\mathbf{c}_c \\ &+ (\omega_s^2\mathbf{K}_L - \omega^2\mathbf{M}_L)\mathbf{c}_s + \omega\mathbf{S}_b\mathbf{w}_c = \mathbf{0}.\end{aligned} \tag{33}$$

The explicit form of elements of the non-linear matrix $\mathbf{D}_{NL}^e(\mathbf{c}_{ce}, \mathbf{c}_{se})$, which is the counterpart of the $\mathbf{D}_{NL}(\mathbf{c}_c, \mathbf{c}_s)$ matrix on a strip level, is given below:

in Case 1

$$\begin{aligned}d_{11} &= \frac{\gamma_e d_e l}{p_e}\left[\frac{1}{5}c_{ca}c_{sa} + \frac{1}{20}(c_{ca}c_{sb} + c_{cb}c_{sa}) + \frac{1}{30}c_{cb}c_{sb}\right], \\ d_{12} = d_{21} &= \frac{\gamma_e d_e l}{p_e}\left[\frac{1}{20}c_{ca}c_{sa} + \frac{1}{30}(c_{ca}c_{sb} + c_{cb}c_{sa}) + \frac{1}{20}c_{cb}c_{sb}\right], \\ d_{22} &= \frac{\gamma_e d_e l}{p_e}\left[\frac{1}{30}c_{ca}c_{sa} + \frac{1}{20}(c_{ca}c_{sb} + c_{cb}c_{sa}) + \frac{1}{5}c_{cb}c_{sb}\right],\end{aligned} \tag{34a}$$

in Case 2

$$d_{11} = \frac{\gamma_e d_e l}{p_e}c_c c_s. \tag{34b}$$

Above, the c_{ca}, c_{cb} and c_{sa}, c_{sb} symbols denote the elements of the $\mathbf{c}_{ce}$ and $\boldsymbol{c}_{se}$ vectors respectively.

For convenience, and using the following notation:

$$\tilde{\mathbf{M}}_b = \begin{bmatrix}\mathbf{M}_b & \mathbf{0} \\ \mathbf{0} & \mathbf{M}_b\end{bmatrix}, \quad \tilde{\mathbf{K}}_b = \begin{bmatrix}\mathbf{K}_b & \mathbf{0} \\ \mathbf{0} & \mathbf{K}_b\end{bmatrix}, \quad \tilde{\mathbf{D}}_b = \begin{bmatrix}\mathbf{0} & \mathbf{D}_b \\ -\mathbf{D}_b & \mathbf{0}\end{bmatrix}, \quad \tilde{\mathbf{S}}_L = \begin{bmatrix}\mathbf{S}_L & \mathbf{0} \\ \mathbf{0} & \mathbf{S}_L\end{bmatrix}, \tag{35}$$

$$\tilde{\mathbf{M}}_L = \begin{bmatrix}\mathbf{M}_L & \mathbf{0} \\ \mathbf{0} & \mathbf{M}_L\end{bmatrix}, \quad \tilde{\mathbf{K}}_L = \begin{bmatrix}\mathbf{K}_L & \mathbf{0} \\ \mathbf{0} & \mathbf{K}_L\end{bmatrix}, \quad \tilde{\mathbf{D}}_L = \begin{bmatrix}\mathbf{0} & \mathbf{D}_L \\ -\mathbf{D}_L & \mathbf{0}\end{bmatrix}, \quad \tilde{\mathbf{S}}_b = \begin{bmatrix}\mathbf{0} & \mathbf{S}_b \\ -\mathbf{S}_b & \mathbf{0}\end{bmatrix}, \tag{36}$$

$$\tilde{\mathbf{D}}_{NL} = \begin{bmatrix}\mathbf{0} & \mathbf{D}_{NL}(\mathbf{c}_c, \mathbf{c}_c) + \mathbf{D}_{NL}(\mathbf{c}_s, \mathbf{c}_s) \\ -\mathbf{D}_{NL}(\mathbf{c}_c, \mathbf{c}_c) - \mathbf{D}_{NL}(\mathbf{c}_s, \mathbf{c}_s) & \mathbf{0}\end{bmatrix}, \tag{37}$$

$$\tilde{\mathbf{w}} = col(\mathbf{w}_c, \mathbf{w}_s), \qquad \tilde{\mathbf{c}} = col(\mathbf{c}_c, \mathbf{c}_s), \tag{38}$$

the amplitude equations can be rewritten in the compact form of the first order:

$$\tilde{\mathbf{G}}_b(\tilde{\mathbf{w}}, \tilde{\mathbf{c}}, \omega, \omega_s) = (\tilde{\mathbf{K}}_b - \omega^2 \tilde{\mathbf{M}}_b + \omega \tilde{\mathbf{D}}_b)\tilde{\mathbf{w}} - \omega_s^2 \tilde{\mathbf{S}}_L \tilde{\mathbf{c}} = \mathbf{0}, \tag{39}$$

$$\begin{aligned} \tilde{\mathbf{G}}_L(\tilde{\mathbf{w}}, \tilde{\mathbf{c}}, \omega, \omega_s) = & -\omega \tilde{\mathbf{S}}_b \tilde{\mathbf{w}} \\ & + [\omega_s^2 \tilde{\mathbf{K}}_L - \omega^2 \tilde{\mathbf{M}}_L - \omega \omega_s \tilde{\mathbf{D}}_L + \tfrac{3}{4} \omega^3 \omega_s^{-1} \tilde{\mathbf{D}}_{NL}(\tilde{\mathbf{c}}, \tilde{\mathbf{c}})]\tilde{\mathbf{c}} = \mathbf{0}. \end{aligned} \tag{40}$$

The most compact form of amplitude equations is given by

$$\tilde{\mathbf{G}}(\omega, \omega_s, \mathbf{a}) = \tilde{\mathbf{K}}(\omega, \omega_s, c)\tilde{\mathbf{a}} = \mathbf{0}, \tag{41}$$

where

$$\tilde{\mathbf{K}}(\omega, \omega_s, \tilde{\mathbf{c}}) = \begin{bmatrix} (\tilde{\mathbf{K}}_b - \omega^2 \tilde{\mathbf{M}}_b + \omega \tilde{\mathbf{D}}_b) & -\omega_s^2 \tilde{\mathbf{S}}_L \\ -\omega \tilde{\mathbf{S}}_b & (\omega_s^2 \tilde{\mathbf{K}}_L - \omega^2 \tilde{\mathbf{M}}_L - \omega \omega_s \tilde{\mathbf{D}}_L + \tfrac{3}{4} \omega^3 \omega_s^{-1} \tilde{\mathbf{D}}_{NL}(\tilde{\mathbf{c}}, \tilde{\mathbf{c}})) \end{bmatrix},$$

$$\tilde{\mathbf{G}} = col(\tilde{\mathbf{G}}_b, \tilde{\mathbf{G}}_L), \qquad \tilde{\mathbf{a}} = col(\tilde{\mathbf{w}}, \tilde{\mathbf{c}}). \tag{42}$$

The $\tilde{\mathbf{G}}$ vector vanishes in an equilibrium state.

5. CONTINUATION PROCEDURE

The amplitude equation (41) is algebraic, homogenous and non-linear. Due to non-linearity the solution of this type of equation, for the given value of U, is not a trivial problem, so it is necessary to apply an advanced procedure. Moreover, one is often interested in the solution of the considered problem for different values of mean wind velocity U taken from an assumed range.

For these reasons, equations (30)–(33) are solved for different ω_s (or U due to the relation $\omega_s = 2\pi SU/D$) using the continuation method. The method has been widely described in a book by Seydel [23]. It is very well oriented as a procedure for solving the system of equations with a parameter. In this article the wind velocity is chosen as the main parameter. It is easy to verify, one basis of equation (41), that $\tilde{\mathbf{a}} = \mathbf{0}$ is the solution of the amplitude equations for all U. Moreover, if ω and $\tilde{\mathbf{a}} \neq \mathbf{0}$ are, for a particular value of U, the solution of the amplitude equation then ω, and $-\tilde{\mathbf{a}}$ are also the solution. It follows from the facts that the amplitude equation is homogeneous and the non-linear matrices of the type $\mathbf{D}_{NL}, (\mathbf{c}_c, \mathbf{c}_s)$ are quadratic functions of amplitudes of the lift coefficients $\mathbf{c}_c$ and $\mathbf{c}_s$.

The trivial solution could be represented on the amplitude of vibration—wind velocity diagram or the amplitude of lift coefficient—wind velocity diagram as a line coinciding with the ω_s (or U) axis. This is the line on which the bifurcation point exists. An additional branch representing the non-trivial solution of equation (38) emanates from the bifurcation point. This branch has been determined by means of the continuation method.

The bifurcation analysis of the original Hartlen–Currie model described by equations (1) and (2) has already been presented in reference [24] by Poore and Al-Rawi. It has been found that the primary bifurcation points exist on the response curve and the non-trivial solutions emanate from these points.

In the case of the system with many degrees of freedom the primary bifurcation points could be determined as described below. At the beginning, the equations of motion (25)

and (26) are written as a system of four first order matrix differential equations. Let $\mathbf{x}_1(t) = \mathbf{w}(t)$, $\mathbf{x}_2(t) = \dot{\mathbf{w}}(t)$, $\mathbf{x}_3(t) = \mathbf{c}(t)$ and $\mathbf{x}_4(t) = \dot{\mathbf{c}}(t)$. Now the equation of motion can be written in the following matrix form:

$$\dot{\mathbf{x}}(t) = \mathbf{A}(\mathbf{x}(t))\mathbf{x}(t), \tag{43}$$

where $\mathbf{x}(t) = col(\mathbf{x}_1(t), \mathbf{x}_2(t), \mathbf{x}_3(t), \mathbf{x}_4(t))$ and

$$\mathbf{A}(\mathbf{x}(t)) = \begin{bmatrix} \mathbf{0} & \mathbf{I} & \mathbf{0} & \mathbf{0} \\ -\mathbf{M}_b^{-1}\mathbf{K}_b & -\mathbf{M}_b^{-1}\mathbf{D}_b & \omega_s^2\mathbf{M}_b^{-1}\mathbf{S}_L & \mathbf{0} \\ \mathbf{0} & \mathbf{0} & \mathbf{0} & \mathbf{I} \\ \mathbf{0} & -\mathbf{M}_L^{-1}\mathbf{S}_L & -\omega_s^2\mathbf{M}_L^{-1}\mathbf{K}_L & \mathbf{M}_L^{-1}(\omega_s\mathbf{D}_L - \omega_s^{-1}\mathbf{D}_{NL}(\mathbf{x}_4, \mathbf{x}_4)) \end{bmatrix}. \tag{44}$$

The one steady state solution of equation (43) is $\mathbf{x} = \mathbf{0}$. The stability of this steady state is based on the exponential growth or decay of solutions of the following perturbation equation:

$$\delta\dot{\mathbf{x}}(t) = \mathbf{A}\delta\mathbf{x}(t), \tag{45}$$

where $\delta\mathbf{x}(t)$ is the small perturbation of steady state solutions and the matrix $\mathbf{A}$ which has the form

$$\mathbf{A} = \begin{bmatrix} \mathbf{0} & \mathbf{I} & \mathbf{0} & \mathbf{0} \\ -\mathbf{M}_b^{-1}\mathbf{K}_b & -\mathbf{M}_b^{-1}\mathbf{D}_b & \omega_s^2\mathbf{M}_b^{-1}\mathbf{S}_L & \mathbf{0} \\ \mathbf{0} & \mathbf{0} & \mathbf{0} & \mathbf{I} \\ \mathbf{0} & -\mathbf{M}_L^{-1}\mathbf{S}_L & -\omega_s^2\mathbf{M}_L^{-1}\mathbf{K}_L & \mathbf{M}_L^{-1}\omega_s\mathbf{D}_L \end{bmatrix}. \tag{46}$$

It is well known that if the real parts of all eigenvalues of $\mathbf{A}$ are negative, the trivial solution is stable, whereas if any of the real parts are positive, the trivial solution is unstable. The bifurcation point occurs when there is a zero eigenvalue or whenever there is a pair of complex conjugate purely imaginary eigenvalues. In the latter case we have the Hopf bifurcation point from which the periodic solution emanates as one of the system parameters (here the mean wind velocity) varies. By holding the remaining system parameter fixed and varying the wind speed gradually, the stability of trivial solution can be checked and in this way the critical wind speed U_c at which the $\mathbf{A}$ matrix has a pair of purely imaginary eigenvalues can be determined.

Unfortunately, for the considered problem, the numerical experiments show that it is very difficult to determine the non-trivial branch of the periodic solution if the primary bifurcation point is taken as the starting point of the continuation procedure. Furthermore, outside the synchronization region the amplitudes of vibration are small and close to the ones obtained on basis of the linear theory. For these reasons the initial approximation of the first point on the response curve can be chosen as follows. The initial value of shedding frequency ω_s is taken far away from the synchronization range and the initial value of ω is equal to ω_s. The chosen initial values of amplitude vectors are

$$\mathbf{w}_c = \mathbf{w}_s = \mathbf{c}_c = \mathbf{0}, \qquad c_{si} = \sqrt{\frac{3}{4\gamma}D_{L,ii}}, \tag{47}$$

where $D_{L,ii}$ and c_{si} are the ith diagonal element of the $\mathbf{D}_L$ matrix and the ith element of the $\mathbf{c}_s$ vector respectively. The initial values of the $\mathbf{c}_s$ vector are approximately equal to the amplitude of the lift factor in the case of wind acting on the motionless rigid finite elements (see also reference [5]). The Newton method is used to determine accurately the first point on the response curve.

Having one point on the response curve one can determine the next one using the continuation method. In comparison with the typical continuation procedure applied to the system of non-linear equations, the one used in this paper is different in some important details and that is why it is described briefly below.

The continuation method is incremental-iterative. The solutions of the matrix amplitude equation are represented by a sequence of vortex-shedding frequencies, the frequencies of periodic responses and the amplitudes vectors, i.e. ${}^m\omega_s, {}^m\omega, {}^m\tilde{\mathbf{a}}$ for $m = 1, 2, \ldots$. For any incremental step, the ${}^m\tilde{\mathbf{a}}$ vector and ${}^m\omega_s, {}^m\omega$ of the proceeding step m is assumed to be given. The purpose of the incremental process is to find the increments of the above-mentioned quantities denoted by $\Delta\omega_s, \Delta\omega, \Delta\tilde{\mathbf{a}}$, which can be accumulated to yield

$$ {}^{m+1}\omega_s = {}^m\omega_s + \Delta\omega_s, \qquad {}^{m+1}\omega = {}^m\omega + \Delta\omega, \qquad {}^{m+1}\tilde{\mathbf{a}} = {}^m\tilde{\mathbf{a}} + \Delta\tilde{\mathbf{a}}. \tag{48} $$

The last equation can be also rewritten in the form

$$ {}^{m+1}\tilde{\mathbf{w}} = {}^m\tilde{\mathbf{w}} + \Delta\tilde{\mathbf{w}}, \qquad {}^{m+1}\tilde{\mathbf{c}} = {}^m\tilde{\mathbf{c}} + \Delta\tilde{\mathbf{c}}. \tag{49} $$

In equation (41) there are $(n+1)$ unknowns (i.e., $\omega, \tilde{\mathbf{w}}$ and $\tilde{\mathbf{c}}$) and the main parameter ω_s. However, since the considered dynamic system is autonomous, one of the Fourier coefficients in the function describing the steady state solution can be fixed. For this reason, it is assumed, without loss of generality, that one element of the $\tilde{\mathbf{w}}$ vector, say $\tilde{w}_k$, is equal to zero and we can write the following equation:

$$ \tilde{w}_k = 0. \tag{50} $$

Furthermore, following the continuation method described for example by Seydel [23] the constraints equation is added to the matrix amplitude equation in the form proposed by Crisfield [25]

$$ \Delta\tilde{\mathbf{w}}^{\mathrm{T}}\Delta\tilde{\mathbf{w}}/\mu_b^2 + \Delta\tilde{\mathbf{c}}^{\mathrm{T}}\Delta\tilde{\mathbf{c}}/\mu_L^2 = (\Delta s)^2, \tag{51} $$

where Δs is the increment of the arc-length s, μ_b and μ_L are some scaling parameters. As before the Δ symbol means the increment of succeeding quantity.

Because of non-linearity the set of non-linear equations (41), (50) and (51) can be solved with respect to $\omega_s, \omega, \tilde{\mathbf{a}}$ only by an iterative procedure. Suppose, after the iteration i, one knows some approximation of the solution denoted by $\omega_s^i, \omega^i, \tilde{\mathbf{a}}^i$. The iteration change of the frequencies increments $\delta\omega_s, \delta\omega$ and the $\delta\tilde{\mathbf{a}}$ vector of amplitude increments are governed by the following equation:

$$ \tilde{\mathbf{G}}_a(\tilde{\mathbf{a}}^i, \omega_s^i, \omega^i)\delta\tilde{\mathbf{a}} = -\tilde{\mathbf{G}}(\tilde{\mathbf{a}}^i, \omega_s^i, \omega^i) - \tilde{\mathbf{G}}_s(\tilde{\mathbf{a}}^i, \omega_s^i, \omega^i)\delta\omega_s - \tilde{\mathbf{G}}_\omega(\tilde{\mathbf{a}}^i, \omega_s^i, \omega^i)\delta\omega, \tag{52} $$

where $\tilde{\mathbf{G}}_a$ is the matrix of the first derivatives of the $\tilde{\mathbf{G}}$ vector with respect to $\tilde{\mathbf{a}}$ and $\tilde{\mathbf{G}}_s, \tilde{\mathbf{G}}_\omega$ are the vectors of the first derivatives of $\tilde{\mathbf{G}}$ with respect to ω_s and ω respectively. The explicit form of the above quantities will be given in the next section.

Moreover, we can write

$$ \delta\tilde{w}_k = 0, \tag{53} $$

Condition (53) is used to remove $\delta\tilde{w}_k$ from a set of unknowns and to modify the incremental equation (52). The kth column of the $\tilde{\mathbf{G}}_a$ matrix which is multiplied by $\delta\tilde{w}_k$ is removed and the $\tilde{\mathbf{G}}_s$ vector is introduced in its place. Also the $\tilde{\mathbf{a}}$ vector of unknowns is modified in such a way that $\delta\omega_s$ is introduced in a place of $\delta\tilde{w}_k$. Denoting the $\tilde{\mathbf{G}}_a$ matrix and the $\tilde{\mathbf{a}}$ vector after modification by $\tilde{\mathbf{G}}_{am}$ and $\tilde{\mathbf{a}}_m$ we can rewrite equation (52) in the form

$$ \tilde{\mathbf{G}}_{am}(\tilde{\mathbf{a}}^i, \omega_s^i, \omega^i)\delta\tilde{\mathbf{a}}_m = -\tilde{\mathbf{G}}(\tilde{\mathbf{a}}^i, \omega_s^i, \omega^i) - \tilde{\mathbf{G}}_\omega(\tilde{\mathbf{a}}^i, \omega_s^i, \omega^i)\,\delta\omega. \tag{54} $$

The $\delta\tilde{\mathbf{a}}_m$ vector can be written as a sum of two components

$$\delta\tilde{\mathbf{a}}_m = \delta\tilde{\mathbf{a}}_{mr} + \delta\tilde{\mathbf{a}}_{m\omega}\delta\omega, \tag{55}$$

where the first component represents the influences of the residual vector and the second one is due to the unit change of the frequency of steady state vibration. The $\delta\tilde{\mathbf{a}}_{mr}$ and $\delta\tilde{\mathbf{a}}_{m\omega}$ vectors are determined by using the following relations:

$$\delta\tilde{\mathbf{a}}_{mr} = -\tilde{\mathbf{G}}_{am}^{-1}(\tilde{\mathbf{a}}^i, \omega_s^i, \omega^i)\tilde{\mathbf{G}}(\tilde{\mathbf{a}}^i, \omega_s^i, \omega^i), \tag{56}$$

$$\delta\tilde{\mathbf{a}}_{m\omega} = -\tilde{\mathbf{G}}_{am}^{-1}(\tilde{\mathbf{a}}^i, \omega_s^i, \omega^i)\tilde{\mathbf{G}}_{\omega}(\tilde{\mathbf{a}}^i, \omega_s^i, \omega^i). \tag{57}$$

Having $\delta\tilde{\mathbf{a}}_{mr}$ and $\delta\tilde{\mathbf{a}}_{m\omega}$ we can easily form the $\delta\tilde{\mathbf{a}}_r = col(\delta\tilde{\mathbf{w}}_r, \delta\tilde{\mathbf{c}}_r)$ and $\delta\tilde{\mathbf{a}}_{\omega} = col(\delta\tilde{\mathbf{w}}_{\omega}, \delta\tilde{\mathbf{c}}_{\omega})$ vectors. The iterative change of shedding frequency due to residuals $\delta\omega_{sr}$ and due to the unit change of frequency of vibration $\delta\omega_{\omega}$ is also determined. The total iterative change of $\delta\omega_s$ is given by

$$\delta\omega_s = \delta\omega_{sr} + \delta\omega_{s\omega}\delta\omega. \tag{58}$$

The unknown iterative change of frequency of steady state vibration $\delta\omega$ is determined in the usual way. Substituting the total increment of $\tilde{\mathbf{a}}$ up to the $(i+1)$th iteration given by $\Delta\tilde{\mathbf{a}}^{i+1} = \Delta\tilde{\mathbf{a}}^i + \delta\tilde{\mathbf{a}}$ into constraints equation (51) gives the following equation with respect to $\delta\omega$:

$$a_1\delta\omega^2 + a_2\delta\omega + a_3 = 0, \tag{59}$$

where

$$a_1 = \delta\tilde{\mathbf{w}}_{\omega}^{\mathrm{T}}\delta\tilde{\mathbf{w}}_{\omega}/\mu_b^2 + \delta\tilde{\mathbf{c}}_{\omega}^{\mathrm{T}}\delta\tilde{\mathbf{c}}_{\omega}/\mu_c^2,$$

$$a_2 = 2(\Delta\tilde{\mathbf{w}}^i + \delta\tilde{\mathbf{w}}_r)^{\mathrm{T}}\delta\tilde{\mathbf{w}}_{\omega}/\mu_b^2 + 2(\Delta\tilde{\mathbf{c}}^i + \delta\tilde{\mathbf{c}}_r)^{\mathrm{T}}\delta\tilde{\mathbf{c}}_{\omega}/\mu_c^2,$$

$$a_3 = (\Delta\tilde{\mathbf{w}}^l + \delta\tilde{\mathbf{w}}_r)^{\mathrm{T}}(\Delta\tilde{\mathbf{w}}^i + \delta\tilde{\mathbf{w}}_r)/\mu_b^2 + (\Delta\tilde{\mathbf{c}}^i + \delta\tilde{\mathbf{c}}_r)^{\mathrm{T}}(\Delta\tilde{\mathbf{c}}^i + \delta\tilde{\mathbf{c}}_r)/\mu_c^2 - \Delta s^2. \tag{60}$$

In equation (59), the increment $\delta\omega$, which gives a positive value of $(\Delta\tilde{\mathbf{a}}^{i+1})^{\mathrm{T}}\Delta\tilde{\mathbf{a}}^i$, is taken as the non-trivial solution to avoid doubling back on the response curve. If both solutions give negative or positive values to $(\Delta\tilde{\mathbf{a}}^{i+1})^{\mathrm{T}}\Delta\tilde{\mathbf{a}}^i$, the corresponding incremental step is restarted automatically with the arc-length reduced to half. Also, in the case of negative discriminant of equation (59), the same procedure is followed. To prevent the number of iterations from being too large, a maximum number of iterations is set. If the number of iteration exceeds it, the incremental step is restarted according to the same procedure as before.

A new approximation of the solution of the matrix amplitude equation is given by

$$\Delta\tilde{\mathbf{a}}^{i+1} = \Delta\tilde{\mathbf{a}}^i + \delta\tilde{\mathbf{a}}, \qquad \Delta\omega_s^{i+1} = \Delta\omega_s^i + \delta\omega_s, \qquad \Delta\omega^{i+1} = \Delta\omega^i + \delta\omega,$$

$$\tilde{\mathbf{a}}^{i+1} = {}^m\tilde{\mathbf{a}} + \Delta\tilde{\mathbf{a}}^{i+1}, \qquad \omega_s^{i+1} = {}^m\omega_s + \Delta\omega_s^{i+1}, \qquad \omega^{i+1} = {}^m\omega + \Delta\omega^{i+1}. \tag{61}$$

The iterations are repeated until the assumed accuracy of calculations is reached.

The existence of critical points on the response curve can be checked in a similar way as is described in reference [26].

6. DERIVATION OF $\tilde{\mathbf{G}}_a$ MATRIX AND $\tilde{\mathbf{G}}_s$ AND $\tilde{\mathbf{G}}_{\omega}$ VECTORS

Taking into account relations (30)–(33) as a starting point one can easily verify that the $\tilde{\mathbf{G}}_s$ and $\tilde{\mathbf{G}}_{\omega}$ vectors (i.e., the vectors of the first derivatives of $\tilde{\mathbf{G}}$ with respect to ω_s and ω

respectively) can be written in the following form:

$$\tilde{\mathbf{G}}_s = \begin{bmatrix} -2\omega_s \mathbf{S}_L \mathbf{c}_c \\ -2\omega_s \mathbf{S}_L \mathbf{c}_s \\ 2\omega_s \mathbf{K}_L \mathbf{c}_c - \omega \mathbf{D}_L \mathbf{c}_s - \frac{3}{4}\omega^3 \omega_s^{-2}[\mathbf{D}_{NL}(\mathbf{c}_c, \mathbf{c}_c) + \mathbf{D}_{NL}(\mathbf{c}_s, \mathbf{c}_s)]\mathbf{c}_s \\ \omega \mathbf{D}_L \mathbf{c}_c + \frac{3}{4}\omega^3 \omega_s^{-2}[\mathbf{D}_{NL}(\mathbf{c}_c, \mathbf{c}_c) + \mathbf{D}_{NL}(\mathbf{c}_s, \mathbf{c}_s)]\mathbf{c}_c + 2\omega_s \mathbf{K}_L \mathbf{c}_s \end{bmatrix}, \tag{62}$$

$$\tilde{\mathbf{G}}_\omega = \begin{bmatrix} -2\omega \mathbf{M}_b \mathbf{w}_c + \mathbf{D}_b \mathbf{w}_s \\ -\mathbf{D}_b \mathbf{w}_c - 2\omega \mathbf{M}_b \mathbf{w}_s \\ -2\omega \mathbf{M}_L \mathbf{c}_c - \omega_s \mathbf{D}_L \mathbf{c}_s + \frac{9}{4}\omega^2 \omega_s^{-1}[\mathbf{D}_{NL}(\mathbf{c}_c, \mathbf{c}_c) + \mathbf{D}_{NL}(\mathbf{c}_s, \mathbf{c}_s)]\mathbf{c}_s - \mathbf{S}_b \mathbf{w}_s \\ \omega_s \mathbf{D}_L \mathbf{c}_c - \frac{9}{4}\omega^2 \omega_s^{-1}[\mathbf{D}_{NL}(\mathbf{c}_c, \mathbf{c}_c) + \mathbf{D}_{NL}(\mathbf{c}_s, \mathbf{c}_s)]\mathbf{c}_c - 2\omega \mathbf{M}_L \mathbf{c}_s + \mathbf{S}_b \mathbf{w}_c \end{bmatrix}. \tag{63}$$

The differentiation of non-linear parts of equations (32) and (33) needs particular attention when we derive the elements of the $\tilde{\mathbf{G}}_a$ matrix. The non-linear part of equation (32) is

$$\mathbf{F}_c(\mathbf{c}_c, \mathbf{c}_s) = \tfrac{3}{4}\omega^3 \omega_s^{-1}[\mathbf{D}_{NL}(\mathbf{c}_c, \mathbf{c}_c) + \mathbf{D}_{NL}(\mathbf{c}_s, \mathbf{c}_s)]\mathbf{c}_s \tag{64}$$

and the directional increments of this function can be written as

$$\frac{\delta \mathbf{F}_c(\mathbf{c}_c, \mathbf{c}_s)}{\delta \mathbf{c}_c} = \frac{\partial \mathbf{F}_c(\mathbf{c}_c, \mathbf{c}_s)}{\partial \mathbf{c}_c}\delta \mathbf{c}_c = \frac{3}{4}\omega^3 \omega_s^{-1} \frac{\delta \mathbf{D}_{NL}(\mathbf{c}_c, \mathbf{c}_c)}{\delta \mathbf{c}_c}\mathbf{c}_s, \tag{65}$$

$$\frac{\delta \mathbf{F}_c(\mathbf{c}_c, \mathbf{c}_s)}{\delta \mathbf{c}_s} = \frac{\partial \mathbf{F}_c(\mathbf{c}_c, \mathbf{c}_s)}{\partial \mathbf{c}_s}\delta \mathbf{c}_s = \frac{3}{4}\omega^3 \omega_s^{-1}\left\{[\mathbf{D}_{NL}(\mathbf{c}_c, \mathbf{c}_c) + \mathbf{D}_{NL}(\mathbf{c}_s, \mathbf{c}_s)]\delta \mathbf{c}_s + \frac{\delta \mathbf{D}_{NL}(\mathbf{c}_s, \mathbf{c}_s)}{\delta \mathbf{c}_s}\mathbf{c}_s\right\}. \tag{66}$$

The terms like $(\delta \mathbf{D}_{NL}(\mathbf{c}_c, \mathbf{c}_c)/\delta \mathbf{c}_c)\mathbf{c}_s$ appearing in relations (65) and (66) must be derived on a strip level. Taking into consideration the definition of the $\mathbf{D}^e_{NL}(\mathbf{c}_{ce}, \mathbf{c}_{ce})$ matrix given below

$$\mathbf{D}^e_{NL}(\mathbf{c}_{ce}, \mathbf{c}_{ce}) = \frac{\gamma_e d_e}{p_e}\int_0^l \mathbf{N}_L^{\mathrm{T}}(x)\mathbf{c}_{ce}\mathbf{c}_{ce}^{\mathrm{T}}\mathbf{N}_L(x)\mathbf{N}_L(x)\mathbf{N}_L^{\mathrm{T}}(x)\,\mathrm{d}x \tag{67}$$

and noting that the terms like $\mathbf{N}_L^{\mathrm{T}}(x)\mathbf{c}_{ce}\mathbf{c}_{ce}^{\mathrm{T}}\mathbf{N}_L(x) = \mathbf{c}_{ce}^{\mathrm{T}}\mathbf{N}_L(x)\mathbf{N}_L^{\mathrm{T}}(x)\mathbf{c}_{ce}$ are scalars the following simple result is obtained

$$\frac{\delta \mathbf{D}^e_{NL}(\mathbf{c}_{ce}, \mathbf{c}_{ce})}{\delta \mathbf{c}_{ce}}\mathbf{c}_{se} = 2\mathbf{D}^e_{NL}(\mathbf{c}_{se}, \mathbf{c}_{ce})\delta \mathbf{c}_{ce}. \tag{68}$$

Now relations (65) and (66) can be rewritten in the form

$$\frac{\delta \mathbf{F}_c(\mathbf{c}_c, \mathbf{c}_s)}{\delta \mathbf{c}_c} = \frac{3}{2}\omega^3 \omega_s^{-1}\mathbf{D}_{NL}(\mathbf{c}_s, \mathbf{c}_c)\delta \mathbf{c}_c, \tag{69}$$

$$\frac{\delta \mathbf{F}_c(\mathbf{c}_c, \mathbf{c}_s)}{\delta \mathbf{c}_s} = \frac{3}{4}\omega^3 \omega_s^{-1}[\mathbf{D}_{NL}(\mathbf{c}_c, \mathbf{c}_c) + 3\mathbf{D}_{NL}(\mathbf{c}_s, \mathbf{c}_c)]\delta \mathbf{c}_s. \tag{70}$$

In a similar way, one can analyze the non-linear part of equation (33).

Finally, the $\tilde{\mathbf{G}}_a$ matrix can be written in the following form:

$$\tilde{\mathbf{G}}_a = \begin{bmatrix} \mathbf{G}_{11} & \mathbf{G}_{12} & \mathbf{G}_{13} & \mathbf{G}_{14} \\ \mathbf{G}_{21} & \mathbf{G}_{22} & \mathbf{G}_{23} & \mathbf{G}_{24} \\ \mathbf{G}_{31} & \mathbf{G}_{32} & \mathbf{G}_{33} & \mathbf{G}_{34} \\ \mathbf{G}_{41} & \mathbf{G}_{42} & \mathbf{G}_{43} & \mathbf{G}_{44} \end{bmatrix}, \tag{71}$$

where the $\mathbf{G}_{ij}$ submatrices are defined below

$$\begin{aligned}
&\mathbf{G}_{11} = \mathbf{K}_b - \omega^2\mathbf{M}_b, \qquad \mathbf{G}_{12} = \omega\mathbf{D}_b, \qquad \mathbf{G}_{13} = -\omega_s^2\mathbf{S}_L, \qquad \mathbf{G}_{14} = \mathbf{0},\\
&\mathbf{G}_{21} = -\omega\mathbf{D}_b, \qquad \mathbf{G}_{22} = \mathbf{K}_b - \omega^2\mathbf{M}_b, \qquad \mathbf{G}_{23} = \mathbf{0}, \qquad \mathbf{G}_{24} = -\omega_s^2\mathbf{S}_L,\\
&\mathbf{G}_{31} = \mathbf{0}, \qquad \mathbf{G}_{32} = -\omega\mathbf{S}_b, \qquad \mathbf{G}_{33} = \omega_s^2\mathbf{K}_L - \omega^2\mathbf{M}_L + \tfrac{3}{2}\omega^3\omega_s^{-1}\mathbf{D}_{NL}(\mathbf{c}_s, \mathbf{c}_c),\\
&\mathbf{G}_{34} = -\omega\omega_s\mathbf{D}_L + \tfrac{3}{4}\omega^3\omega_s^{-1}[\mathbf{D}_{NL}(\mathbf{c}_c, \mathbf{c}_c) + 3\mathbf{D}_{NL}(\mathbf{c}_s, \mathbf{c}_s)], \qquad \mathbf{G}_{41} = \omega\mathbf{S}_b,\\
&\mathbf{G}_{42} = \mathbf{0}, \qquad \mathbf{G}_{43} = \omega\omega_s\mathbf{D}_L - \tfrac{3}{4}\omega^3\omega_s^{-1}[3\mathbf{D}_{NL}(\mathbf{c}_c, \mathbf{c}_c) + \mathbf{D}_{NL}(\mathbf{c}_s, \mathbf{c}_s)],\\
&\mathbf{G}_{44} = \omega_s^2\mathbf{K}_L - \omega^2\mathbf{M}_L - \tfrac{3}{2}\omega^3\omega_s^{-1}\mathbf{D}_{NL}(\mathbf{c}_s, \mathbf{c}_c).
\end{aligned} \tag{72}$$

7. SOLUTION OF MOTION EQUATIONS BY NEWMARK METHOD

A time integration method is also used to obtain the steady state, periodic vibration of the considered system and to verify the accuracy of the solution given by the harmonic balance method. The well-known version of the Newmark method called the average acceleration method is chosen to integrate the equations of motion. The algorithm of this method is described in this section.

For convenience, equations (25) and (26) are first rewritten in the following compact form:

$$\mathbf{R}(t) = \mathbf{M}\mathbf{a}(t) + \mathbf{D}(\mathbf{v}(t))\mathbf{v}(t) + \mathbf{K}\mathbf{d}(t) = \mathbf{0}, \tag{73}$$

where

$$\mathbf{R} = col(\mathbf{R}_b, \mathbf{R}_L), \qquad \mathbf{d}(t) = col(\mathbf{w}(t), \mathbf{c}(t)), \qquad \mathbf{v}(t) = \dot{\mathbf{d}}(t), \qquad \mathbf{a}(t) = \dot{\mathbf{v}}(t),$$

$$\mathbf{M} = \begin{bmatrix} \mathbf{M}_b & \mathbf{0} \\ \mathbf{0} & \mathbf{M}_L \end{bmatrix}, \qquad \mathbf{K} = \begin{bmatrix} \mathbf{K}_b & -\omega_s^2\mathbf{S}_L \\ \mathbf{0} & \omega_s^2\mathbf{K}_L \end{bmatrix}, \qquad \mathbf{D} = \begin{bmatrix} \mathbf{D}_b & \mathbf{0} \\ -\mathbf{S}_b & -\omega_s\mathbf{D}_L + \omega_s^{-1}\mathbf{D}_{NL}(\mathbf{v}, \mathbf{v}) \end{bmatrix}.$$

The following Newmark formulas:

$$\mathbf{d}_{n+1} = \mathbf{d}_n + \tau\mathbf{v}_n + \tfrac{1}{4}\tau^2(\mathbf{a}_{n+1} + \mathbf{a}_n), \tag{74}$$

$$\mathbf{v}_{n+1} = \mathbf{v}_n + \tfrac{1}{2}\tau(\mathbf{a}_{n+1} + \mathbf{a}_n), \tag{75}$$

gives the system state at time $t_{n+1} = t_n + \tau$, where τ is the small time interval, if the state at t_n (i.e., the $\mathbf{a}_n, \mathbf{v}_n, \mathbf{d}_n$ vectors) and the $\mathbf{a}_{n+1}$ acceleration vector are known. If the equation of motion is understood to be the equilibrium equation at time t_{n+1}, i.e.,

$$\mathbf{R}_{n+1} = \mathbf{M}\mathbf{a}_{n+1} + \mathbf{D}(\mathbf{v}_{n+1})\mathbf{v}_{n+1} + \mathbf{K}\mathbf{d}_{n+1} = \mathbf{0}, \tag{76}$$

the solution of equations (74)–(76) will give the system state at time t_{n+1}. Equation (76) is non-linear and the Newton method is needed to solve it. Equation (76) is treated as non-linear with respect to $\mathbf{a}_{n+1}$ and the incremental equation corresponding to equation (76) has the form

$$\mathbf{M}_t\delta\mathbf{a} = -\mathbf{R}_{n+1}, \tag{77}$$

where

$$\mathbf{M}_t = \frac{\partial\mathbf{R}_{n+1}}{\partial\mathbf{a}_{n+1}} = \mathbf{M} + \frac{\partial\mathbf{D}(\mathbf{v}_{n+1})}{\partial\mathbf{v}_{n+1}}\frac{\partial\mathbf{v}_{n+1}}{\partial\mathbf{a}_{n+1}} + \mathbf{K}\frac{\partial\mathbf{d}_{n+1}}{\partial\mathbf{a}_{n+1}}. \tag{78}$$

Because

$$\frac{\partial \mathbf{v}_{n+1}}{\partial \mathbf{a}_{n+1}} = \frac{1}{2}\tau \mathbf{I}, \qquad \frac{\partial \mathbf{d}_{n+1}}{\partial \mathbf{a}_{n+1}} = \frac{1}{4}\tau^2 \mathbf{I}, \qquad \frac{\partial \mathbf{D}(\mathbf{v}_{n+1})}{\partial \mathbf{v}_{n+1}} = \mathbf{D}_t, \tag{79}$$

where $\mathbf{I}$ is the diagonal matrix and

$$\mathbf{D}_t = \begin{bmatrix} \mathbf{D}_b & \mathbf{0} \\ -\mathbf{S}_b & -\omega_s \mathbf{D}_L + 3\omega_s^{-1}\mathbf{D}_{NL}(\dot{\mathbf{c}}, \dot{\mathbf{c}}) \end{bmatrix} \tag{80}$$

the $\mathbf{M}_t$ matrix is given by

$$\mathbf{M}_t = \mathbf{M} + \tfrac{1}{2}\tau \mathbf{D}_t + \tfrac{1}{4}\tau^2 \mathbf{K}. \tag{81}$$

Starting with the given initial conditions, the system of equations (74)–(76) is solved and the solution of the equation of motion can be determined by applying the above method recurrently for a number of τ intervals. The steady state solution can be obtained in this way as well.

8. PARAMETRIC ANALYSIS

First of all, results obtained for a simply supported beam by using the well-known normal approach and the present method will be compared. The beam is of length $L = 32{\cdot}0\,\text{m}$, the bending rigidity $EJ = 2{\cdot}0 \times 10^9\,\text{N m}^2$ and the diameter cross-section $D = 1{\cdot}0\,\text{m}$ is chosen. The modal damping of the first mode of vibration is equal to 0·2% of critical damping. The beam is divided into 10 identical finite elements. The mean wind speed is equal to U for all finite elements. A brief description of the solution obtained by the normal mode approach is given in Appendix A. The results of the calculations are shown in Figures 1 and 2. In Figure 1, the non-dimensional amplitude of vibration, i.e., $v = w/D$ in the middle of the beam versus non-dimensional frequency of vibration ω/ω_n is presented. ω_n is the first natural frequency of beam. The solid line represents the response curve obtained by means of the finite element method whereas the response curve determined by the normal mode approach is shown as the dashed line. Moreover, in

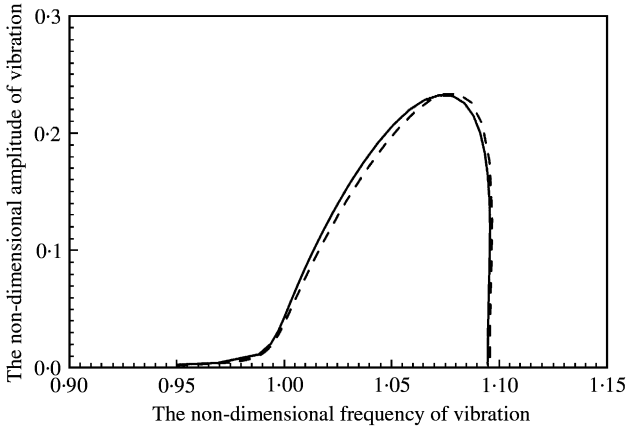

Figure 1. A comparison of the response curves obtained by the normal mode approach (– – – –) and by the present method (——).

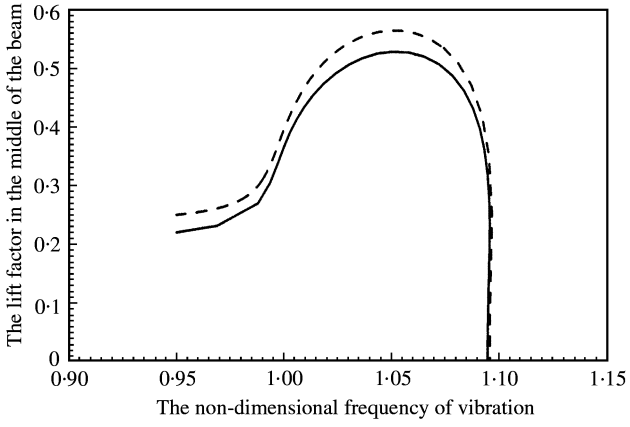

Figure 2. A comparison of the lift factor determined by means of the normal mode approach (– – – –) and by the present method (——).

Figure 2 a similar comparison for the lift coefficient is presented. A good agreement between the results obtained by both methods is visible.

Several numerical analyses for the free-fixed beam with a cylindrical cross-section have been carried out. The following principal data have been chosen: the beam length $L = 32{\cdot}0\,\mathrm{m}$, the bending rigidity $EJ = 2{\cdot}0 \times 10^9\,\mathrm{N\,m^2}$, the diameter of beam cross-section $D = 1{\cdot}2\,\mathrm{m}$. In almost all the cases considered the beam is divided into 10 identical finite elements. The data concerning air are the following: the air density $\rho = 1{\cdot}2\,\mathrm{kg/m^3}$, the Strouhal number $S = 0{\cdot}2$ and the following aerodynamic parameter are chosen: $\alpha = 0{\cdot}02, b = 0{\cdot}4, \gamma = 2/3$.

The first and second natural frequencies of the beam are equal to $\omega_1 = 7{\cdot}2387\,\mathrm{rad/s}$ and $\omega_2 = 45{\cdot}3656\,\mathrm{rad/s}$. The damping matrix of the beam is proportional i.e. $\mathbf{D}_b = \alpha_1 \mathbf{M}_b + \alpha_2 \mathbf{K}_b$ and the factors α_1 and α_2 are determined in such a way that the modal damping of the first and second modes of beam vibrations are equal to 0.1% of critical damping.

The data concerning air are chosen as in a previous case. The mean wind speed is equal to U in a range of first eight elements from the top of beam and equal to zero for others.

The results of calculations obtained by means of the harmonic balance method are shown in Figure 3 (the solid line). The region of the lock-in phenomenon can easily be recognized from this figure. Moreover, the equations of motion are solved using the Newmark method. In this method, having given initial conditions, the equations of motion are integrated numerically until the steady state solution is obtained. The above-mentioned process of integration can be very time consuming, especially when the damping in structures is very small as in the considered case. For example, in the present case the determination of steady state solution by the Newmark method for the chosen mean velocity was from a few hundred to one thousand times slower than the time needed to determine the whole response curve by the continuation method. The calculated results for the steady state solution are also shown in Figure 3 (the small crosses). The perfect agreement between the results obtained by both methods is obvious.

In Figure 4, the convergence of the finite element method, with respect to a number of elements, is presented. The dashed line shows the response curve for the beam divided into

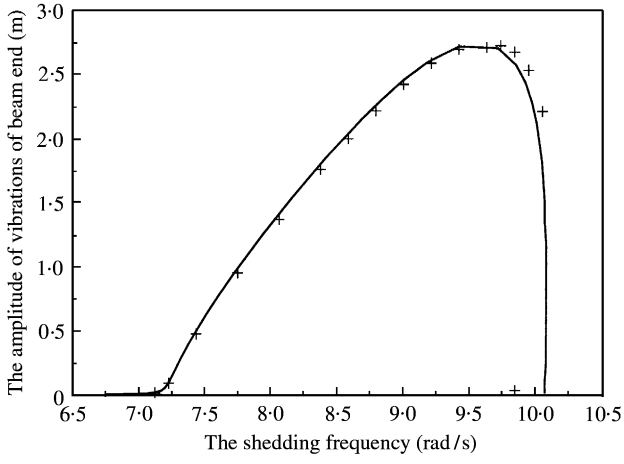

Figure 3. A comparison of results obtained by the Newmark method (+) and the harmonic balance method.

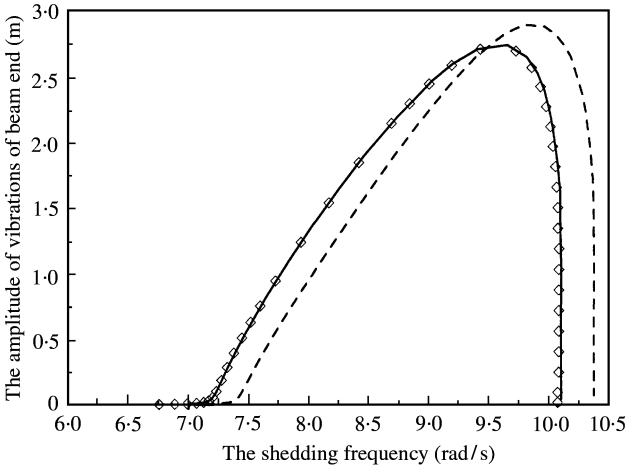

Figure 4. The response curves for beams divided into --- 3, — 5 and –□– 10 finite elements.

three elements. The solution obtained for the beam modelled by five elements is drawn in the solid line. Moreover, the small squares show the results for the beam divided into 10 elements. It is clear that the model with five elements give us the correct results. However, the results described below are obtained for the beam divided into 10 identical elements.

The results of the next analysis are shown in Figure 5, where the response curves obtained for different damping factors are presented. Here, the synchronization range near the first natural frequency of the beam is shown. As can be seen, the influence of damping is very strong both on the amplitudes of vibrations and on the range of synchronization. Furthermore, the results of similar calculations made for the second synchronization region are presented in Figure 6. The second synchronization region is considerably larger than the first one.

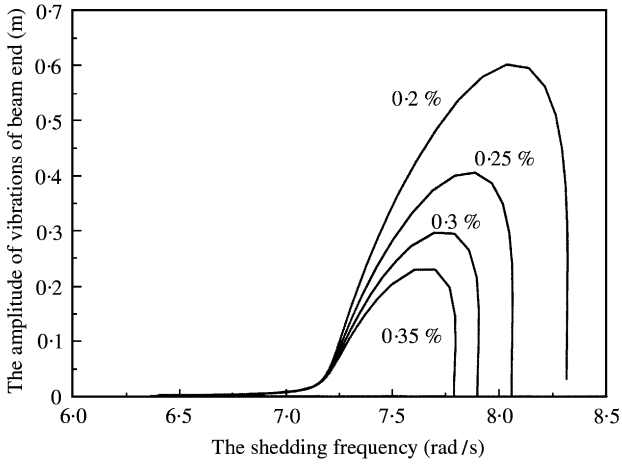

Figure 5. The influence of damping on the amplitude of vibrations and the synchronization range (the shedding frequency near the first natural frequency).

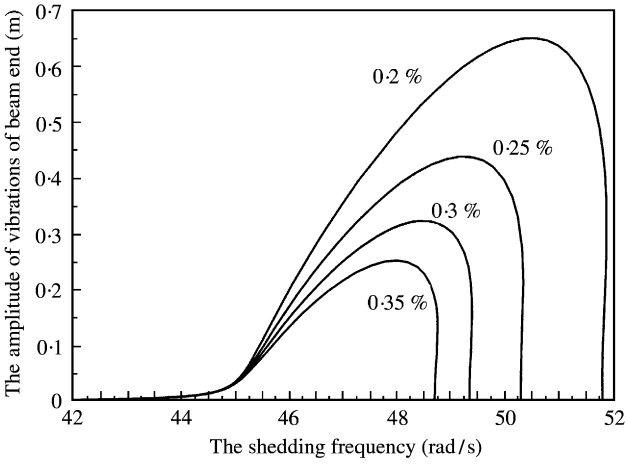

Figure 6. The influence of damping on the amplitude of vibrations and the synchronization range (the shedding frequency near the second natural frequency).

In Figure 7, the response curves calculated for beams with different rigidity and different damping factors are shown. The curves 1 and 2 are obtained if the beam rigidity is $EJ = 2{\cdot}0 \times 10^9\ \mathrm{N\,m^2}$ while the curves 3 and 4 are obtained when the beam rigidity is equal to $EJ = 3{\cdot}0 \times 10^9\ \mathrm{N\,m^2}$. For the beam with greater rigidity the region of synchronization is larger and occurs for greater mean wind speeds.

The influence of the length of the loaded part of the beam in the synchronization region is the subject of the last analysis. In Figure 8, the results of calculations are presented for different loaded finite elements. As it is expected the maximum amplitude of vibration and the range of synchronization increase when more elements are loaded.

All these results indicate that the amplitudes of vibrations grow gradually near the left end of the synchronization region and decrease very fast near the right one.

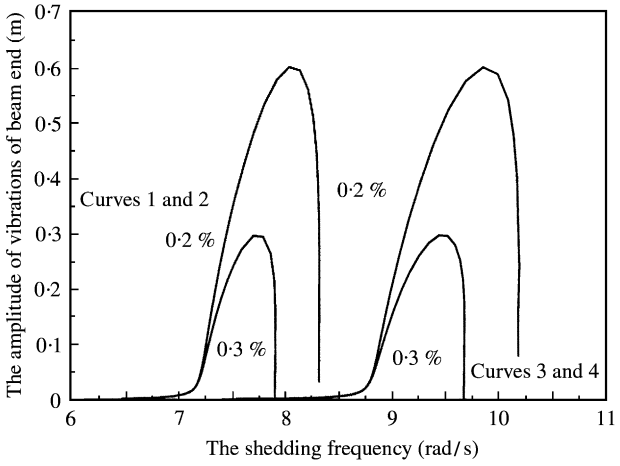

Figure 7. The response curves for beams with different rigidity.

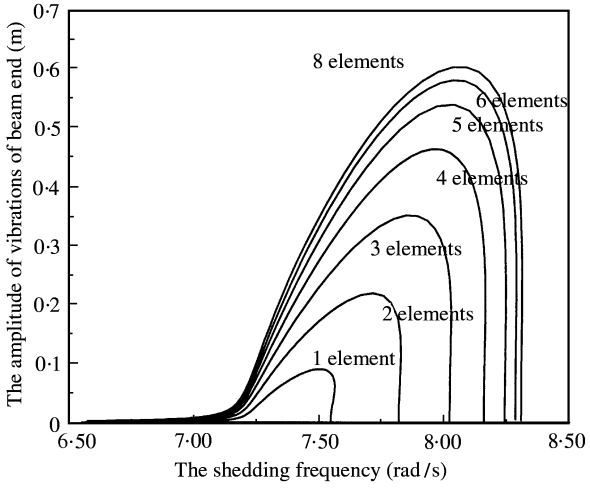

Figure 8. The response curves for the different length of distribution of excitation forces.

9. CONCLUDING REMARKS

In this paper, the computational methods for the analysis of vortex-induced vibration of beams are presented. The main aerodynamic properties of air are taken into account using the model proposed by Hartlen and Currie. The extension of this model to beams treated as multi-degree-of-freedom systems is proposed in this paper. It is believed that the approach presented is a good compromise between the needed effort of calculations and the desired accuracy of the solution of the problem considered. The semi-analytical method (the harmonic balance method) is employed to determine the steady state solution for a set of values of the mean wind velocity. The continuation method used to solve the amplitude equation which makes a parametric analysis of the problem possible. The

validity of the harmonic balance results is confirmed by means of a time integration method. Several numerical analyses were carried out for the beams with cylindrical cross-section. They refer to the convergence of the proposed way of discretization, the influence of damping on the amplitude of vibration and a range of the mean wind velocities when the lock-in phenomenon occurs.

ACKNOWLEDGMENTS

The paper is supported by the Grants No. 7 TO7E 027 12 denoted by the Committee of Scientific Research.

REFERENCES

1. D. Brika and A. Laneville 1993 *Journal of Fluid Mechanics* **250**, 481–508. Vortex-induced vibrations of a long flexible circular cylinder.
2. I. Goswami, R. H. Scanlan and N. P. Jones 1993 *Journal of Engineering Mechanics* **119**, 2270–2287. Vortex-induced vibration of circular cylinders. Part I: experimental data.
3. B. J. Vickery and R. I. Basu 1983 *Journal of Wind Engineering and Industrial Aerodynamics* **12**, 49–73. Across-wind vibrations of structures of circular cross-section. Part I: development of a mathematical model for two-dimensional conditions.
4. A. Flaga 1997 *Journal of Wind Engineering and Industrial Aerodynamics* **69–71**, 331–340. Nonlinear amplitude dependent self-limiting model of lock-in phenomenon at vortex excitation.
5. R. T. Hartlen and I. G. Currie 1970 *Proceedings of the American Society of Civil Engineers* **EM5**, 577–591. Lift oscillator model of vortex-induced vibration.
6. W. D. Iwan and R. D. Blevins 1974 *Journal of Applied Mechanics* **41**, 581–586. A model for vortex induced oscillation of structures.
7. R. Landle 1975 *Journal of Sound and Vibration* **42**, 219–234. A mathematical model for vortex-excited vibrations of bluff bodies.
8. R. A. Skop and O. M. Griffin 1973 *Journal of Sound and Vibration* **41**, 263–274. On a theory for the vortex-excited oscillations of flexible cylindrical structures.
9. H. L. Oey, I. G. Currie and H. J. Leutheusser 1975 *Proceedings of the Fourth International Conference on Wind Eects on Buildings and Structures* (K. J. Eaton, editor) Cambridge: Cambridge University Press, 233–240. On the double-amplitude response of circular cylinders excited by vortex shedding.
10. S. Krenk and S. R. K. Nielsen 1998 *Journal of Engineering Mechanics* **125**, 263–271. Energy balanced double oscillator model for vortex-induced vibrations.
11. E. Simiu and R. H. Scanlan 1978 *Wind Eects on Structures*. New York: Wiley.
12. I. Goswami, R. H. Scanlan and N. P. Jones 1993 *Journal of Engineering Mechanics* **119**, 2270–2287. Vortex-induced vibrations of circular cylinders. II: new model.
13. A. Larsen 1994 *Journal of Engineering Mechanics* **120**, 350–353. Discussion of "Vortex-induced vibrations of circular cylinders. II: new model."
14. H. Ruschaweyh 1982 *Dynamische Windwirkung an Bauwerken*. Wiesbaden und Berlin: Bauverlag Gmbh.
15. H. Barhoush, A. H. Namini and R. A. Skop 1995 *Journal of Sound and Vibration* **184**, 111–127. Vortex shedding analysis by finite elements.
16. F. A. Dul and J. A. Pietrucha 1994 *Proceedings of the East European Conference of Wind Engineering, Warsaw, Poland, July* 1994*, Part* II/I, 67–79. Numerical analysis of continuos models of structures in nonlinear wind flow using the time-marching approach.
17. R. Lewandowski 1996 *Proceedings of the Third European Conference on Structural Dynamics, EURODYN*'96, *Florence*, Italy, 5–8 July (G. Augusti *et al*., editors), Vol. 2, 221–226, Rotterdam: Balkema. Computational formulation for non-linear vortex-induced vibration of beams.
18. E. Simiu and R. H. Scanlan 1996 *Wind eects on structures*. New York: J. Wiley; third edition.
19. K. Yasuda and T. Torii 1987 *JSME International Journal* **30**, 963–969. Multi-mode response of a square membrane.

20. R. LEWANDOWSKI 1994 *Journal of Sound and Vibration* **170**, 577–593. Non-linear free vibrations of beams by the finite element and continuation methods.
21. D. A. EVENSEN 1968 *Journal of the Acoustical Society of America* **44**, 84–89. Influence of nonlinearities on the degenerate vibration modes of a square plate.
22. R. BENAMAR, M. M. K. BENNOUNA and R. G. WHITE 1991 *Journal of Sound and Vibration* **149**, 179–195. The effects of large vibration amplitudes on the mode shapes and natural frequencies of thin elastic structures. Part I: simply supported and clamped–clamped beams.
23. R. SEYDEL 1988 *From Equilibrium to Chaos: Practical Bifurcation and Stability Analysis*. New York: Elsevier.
24. A. B. POORE and A. R. AL-RAWI 1979 *Proceedings of the Fifth International Conference of Wind Engineering, Fort Collins, U.S.A., Pergamon Oxford* 1980, 1073–1083. The dynamical behaviour of the Hartlen–Currie wake oscillator model.
25. M. A. CRISFIELD 1981 *Computers and Structures* **13**, 55–62. A fast incremental/iterative solution procedure that handles snap through.
26. R. LEWANDOWSKI 1997 *International Journal of Solids and Structures* **34**, 1949–1964. Computational formulation for periodic vibration of geometrically nonlinear structures. Part 2: numerical strategy and examples.

APPENDIX A

The solution of the considered problem by means of the normal mode approach is briefly described. The equation of motion of the beam and the equation of motion of the fictitious aerodynamic oscillators are written in the following form:

$$m\ddot{w}(x,t) + c_b\dot{w}(x,t) + EJw_{,xxxx} = \tfrac{1}{2}\rho U^2(x)D(x)c_L(x,t), \tag{A.1}$$

$$\ddot{c}_L(x,t) - \alpha\omega_s c_L(x,t) + \gamma/\omega_s\dot{c}_L^3(x,t) + \omega_s^2 c_L(x,t) = b\omega_n/D(x)\dot{w}(x,t). \tag{A.2}$$

Above, c_b denotes the beam damping factor and ω_n is the chosen natural frequency of beam. The real time t is used in the motion equations instead of the non-dimensional time $\tau = \omega_n t$ used in the original Hartlen–Currie formulation. For this reason ω_n appears on the right side of equation (A.2). Moreover, it is assumed that $U(x) = U = const.$ and $D(x) = D = const.$

The solution of the equations of motion is assumed of the following form:

$$w(x,t) = v(t)/D \sin\frac{n\pi x}{L}, \qquad c_L(x,t) = c(t)\sin\frac{n\pi x}{L}, \tag{A.3}$$

where $v(t)$ and $c(t)$ are the modal coordinates.

Introducing the assumed solution (A.3) into the equations of motion (A.1) and (A.2) and applying the Galerkin method in space, one obtains the following modal equations of motion for the simply supported beam:

$$\begin{aligned} &\ddot{v}(t) + \eta\omega_n\dot{v}(t) + \omega_n^2 v(t) - \omega_s^2 ac(t) = 0,\\ &\ddot{c}(t) - \alpha\omega_s\dot{c}(t) + 3\gamma/(4\omega_s)\dot{c}_L^3(t) + \omega_s^2 c(t) - b\dot{v}(t) = 0, \end{aligned} \tag{A.4}$$

where η is the modal damping of beam and $a = \rho D^3/(8\pi^2 S^2 m)$.

The steady state solution of the modal equations (A.4) is assumed in the form

$$v(t) = v_c\cos\omega t + v_s\sin\omega t, \qquad c(t) = c_c\cos\omega t + c_s\sin\omega t. \tag{A.5}$$

The unknown amplitudes v_c, v_s, c_c and c_s are determined from the following amplitude equations:

$$\begin{aligned}
&(\omega_n^2 - \omega^2)v_c + \eta\omega\omega_n v_s - \omega_s^2 a c_c = 0,\\
&-\eta\omega\omega_n v_c + (\omega_n^2 - \omega^2)v_s - \omega_s^2 a c_s = 0,\\
&(\omega_s^2 - \omega^2)c_c - \omega\omega_s \alpha c_s + \frac{9\omega^3\gamma}{16\omega_s}(c_c^2 + c_s^2)c_s - \omega b v_s = 0,\\
&\omega\omega_s \alpha c_c - \frac{9\omega^3\gamma}{16\omega_s}(c_c^2 + c_s^2)c_c + (\omega_s^2 - \omega^2)c_s + \omega b v_c = 0,
\end{aligned} \tag{A.6}$$

derived by means of the harmonic balance method. The amplitude equations (A.6) can be solved using, for example, the continuation method described in the previous section.